Regulation of BMP and TGFβ signaling pathway in cancer progression

Ren, J.

Chapter 4

Synergistic Reactivation of BMP Signaling by MEK Inhibitor and FK506 Reduces Breast Cancer Metastasis

Jiang Ren*, Yanhong Wang*, Josephine Iaria, Peter ten Dijke and Hong Jian Zhu

Manuscript in submission

*These authors contributed equally

Abstract

Transforming growth factor β (TGFβ)-SMAD3 signaling is a major driving force for cancer metastasis, while bone morphogenetic protein (BMP)-SMAD1/5 signaling can counteract this response. TGFβ-SMAD3 signaling is a major driving force for cancer metastasis, while BMP-SMAD1/5 signaling can counteract this response. We discovered that TGFβ abolished BMP-induced SMAD1/5 activation in the highly-invasive breast cancer MDA-MB-231 cells, but to a less extent in the non-invasive and normal breast cells. This suggests an inverse correlation between BMP signaling and invasiveness of tumor cells and TGFβ signaling acts in a double whammy fashion in driving cancer invasion and metastasis. Sustained ERK activation by TGFβ was specifically observed in MDA-MB-231 cells, and treatment with MEK inhibitor (MEKi) restored BMP signaling. FK506 potently activated BMP, but not TGFβ signaling in breast cancer cells. MEKi or FK506 alone inhibited MDA-MB-231 extravasation in zebrafish cancer model. Importantly, when administrated at suboptimal concentrations MEKi and FK506 strongly synergized in promoting BMP-SMAD1/5 signaling and inhibiting cancer cell extravasation. Furthermore, this combination treatment in a mice tumor model potently inhibited tumor self-seeding, liver and bone metastasis, but not lung and brain metastasis. Combining of MEK1 and FK506, or their analogues, may be explored for clinical development of breast cancer.

Keywords: BMP, Breast cancer metastasis, FK506, TGFβ, U0126

Introduction

Although substantial progress of early diagnosis and molecular target therapy has been achieved in treating the primary niche of breast cancer patients, a dismal fact remains that over 90% of breast cancer-related deaths are caused by metastatic recurrence at distal organs, commonly bone, brain, lung, liver, and lymph nodes. For cells that contribute to effective metastases, they must successively gain the abilities of escaping the primary site, intravasation into the vasculatures, surviving in the circulation, then extravasation and colonization at the target organs [1]. It has been well-established that transforming growth factor β (TGFβ) signaling serves as a major metastasis driver through promoting epithelial-mesenchymal transition (EMT), leading to increased invasion and dissemination of cancer cells, and also through inducing genes that facilitate metastatic colonization [2, 3].

Signaling of other TGFβ family members, *i.e.* bone morphogenetic proteins (BMPs) can have a negative effect on EMT and metastatic colonization, indicating a mutual antagonistic role of TGFβ and BMP signaling in cancer metastasis [4, 5]. Studies showed that the imbalance between them, towards TGFβ signaling [6, 7], as well as BMP antagonists [8, 9] confer the ability of breast cancer cell metastasis. As such, it is worthwhile to interfere with this imbalance artificially; restoring or enhancing BMP signaling activity could be beneficial for reducing metastasis. For instance, activation of BMP4 blocks breast cancer metastasis and BMP4 correlates with good prognosis in patients [10]. Exogenous administration of BMP7 counteracted TGFβ-mediated EMT and inhibited the osteolytic bone metastases of breast cancer cells [11]. BMP-7 inhibited TGFβ-induced expression of integrin αvβ3, which can enhance EMT and expressed strongly in breast cancer cells that metastasize to bone [12].

Signaling by TGFβ family is a paradigm of membrane-to-nucleus pathway. Upon ligand-induced heteromeric complex formation of specific type I and II transmembrane serine/threonine kinase receptors, receptor regulated (R-)SMAD2/3 and SMAD1/5/8, acting downstream of TGFβ and BMP respectively, are phosphorylated by the activated type I receptor. Phosphorylated R-SMADs (pSMADs) form complexes with SMAD4, which can translocate into the nucleus to regulate genes transcription [13-15]. As SMAD4 is the only common partner, one antagonism between TGFβ (-like) and BMP signaling is pSMAD2/3 can compete with pSMAD1/5 for binding SMAD4 [16, 17]. In addition, TGFβ could induce a nonfunctional complex comprising

of phosphorylated SMAD1/5 and SMAD3 resulting in inhibition of BMP response in highly-invasive MDA-MB-231 cells [18].

What's more versatile, TGFβ-regulated responses can be mediated by several non-canonical SMAD pathways, best illustrated in the activation of phosphatidyl inositol (PI)3K/AKT and early response kinase (ERK) mitogen activated protein kinase (MAPK) [19, 20]. Numerous studies have revealed that the SMAD proteins are a critical platform for integrating RTK/MAPK signals with the TGFβ signaling [21]. How non-canonical TGFβ signaling affect TGFβ and BMP crosstalk remains unclear, as well as subsequent effect on cancer metastasis.

In this study, we found TGFβ induced abolishment of the BMP signaling activity in MDA-MB-231 cells. The BMP-SMAD1/5 activation could be restored by MAPK kinase (MEK) inhibitors U0126 or PD98059. Moreover, FK506 was identified as a BMP/SMAD1/5 signaling agonist that inhibited cancer cell extravasation. Notably, suboptimal concentrations of U0126 and FK506 exhibited synergistic effects on restoring BMP signaling both in vitro and in vivo. Furthermore, U0126 and FK506 combination treatment in a strongly cooperative manner reduced extravasation in zebrafish breast cancer model and liver, bone metastasis and tumor self-seeding in mouse breast cancer model. Therefore, future therapies targeting BMP signaling restoration in cancer cells may be worthwhile to be developed for cancer metastasis treatment.

Methods

Cell lines, culture conditions

The human breast cancer cell lines MDA-MB-231 and MCF7, human epidermal carcinoma cell line A431, human head and neck tumor cell line HN5, Madin-Darby canine kidney cell line MDCK, the H-Ras-transformed MDCK (21D1 cells) [22], mouse mammary epithelial cell line NMuMG, and mouse fibroblast cell line NIH3T3 were originally obtained from ATCC (American Type Culture Collection). Doxycycline inducible Ras transformed NIH3T3 fibroblasts [23] and mCherry stable expression MDA-MB-231 cell line had been described before [9, 24]. These cell lines were cultured in Dulbecco's modified Eagle's medium (DMEM, 11965092, ThermoFisher Scientific) supplemented with 10% Fetal Bovine Serum (FBS, 16000044, ThermoFisher Scientific), 100 U/ml Penicillin/Streptomycin (Pen/Strep, 15140148, ThermoFisher Scientific). Human breast epithelial cell line MCF10A [25] was generously provided by Dr. Fred Miller (Barbara Ann Karmanos Cancer Institute, Detroit, USA), and

cultured in DMEM/F12 medium (11039047, ThermoFisher Scientific) supplemented with 5% horse serum (26050088, ThermoFisher Scientific), 20 ng/ml epidermal growth factor (EGF, 01-107, Merck Millipore), 10 mg/ml insulin (91077C, Sigma-Aldrich), 100 ng/ml cholera enterotoxin (C8052, Sigma-Aldrich), and 0.5 mg/ml hydrocortisone (H0135, Sigma-Aldrich) and 100 U/ml Pen/Strep. All cell lines were maintained at 37 °C, 5% CO_2, humidified incubator. All cell lines were monthly tested to verify absence of mycoplasma and human cell lines were authenticated by single nucleotide polymorphism (SNP) analysis.

Cells treatment and small molecule compounds

We obtained recombinant human BMP6/7 (120-06/120-03, PeproTech and from Dr. S. Vukicevics), TGFβ3 (100-36E, PeproTech and A.P. Hinck, University of Pittsburg, USA) and Doxycycline monohydrate (Dox, D1822, Sigma-Aldrich). In certain experiments, cells were received combinational treatments at different priorities with 30 min pretreatment, The compounds that were used in this study: BMP type I receptors inhibitor LDN193189 (SML0559, Sigma-Aldrich) [26], TGFβ type 1 receptor (also termed activin receptor-like kinase (ALK5) inhibitor SB-431542 (S4317, Sigma-Aldrich), MEK inhibitor U0126 (U120, Sigma Aldrich) or PD98059 (9900, Cell Signaling Technology), PI3K inhibitor LY294002 (L9908, Sigma-Aldrich). All small molecule FDA-approved drugs and biologically active compounds were purchased from Sigma-Aldrich, including FK506 (Tacrolimus, F4679). Cells were maintained in serum free medium when receiving treatment, unless otherwise specified.

Adenovirus production

The BMP-SMAD1/5 signaling reporter Ad-Bre-Firefly (F)-luciferase (Luc), TGFβ-SMAD3 signaling reporter Ad-CAGA-Gaussia (G)-Luc, and Wnt signaling reporter Ad-TCF-F-Luc and Ad-CMV-G-Luc adenoviruses were produced and amplified as previously described [27, 28]. Ad-CMV-Flag-SMAD6 viruses were produced similarly for the purpose being infect cultured cells for overexpression of SMAD6 [28].

siRNA-mediated knockdown

MDA-MB-231 cells were transiently transfected with control siRNA (ON-TARGETplus Non-targeting control siRNAs, D-001810-01-05, Dharmacon) or SMAD6 siRNA (SMARTPool, L-015362-00-0010, Dharmacon) using Lipofectamine RNAiMAX (13778030, ThermoFisher

Scientific) according to the manufacturer's protocol. Successful knockdown of SMAD6 was confirmed by western blotting.

Luciferase reporter assay

Ad-Bre-F-Luc/Ad-TCF-F-Luc (multiplicity of infection (MOI): 2000) and Ad-CMV-G-Luc/Ad-CAGA-G-Luc (MOI: 1000) virus infected cells (3000 cells/well approximately) were cultured in a 96-well plate as previously described [28]. Or cells in a 24-well plate, which were seeded 1 day before (5×10^4 cells/well approximately), were co-transfected with 0.1μg TGFβ-SMAD3-inducible $(CAGA)_{12}$ or BMP responsive element (Bre) F-Luc transcriptional reporter transcriptional reporter construct and 0.08 μg β-galactosidase (βgal) expression construct using lipofectamine 3000 (L3000001, ThermoFisher Scientific). After overnight infection or transfection, cells were starved with low serum (0.2%) medium. 8 h later, cells were received conceived treatments. After another overnight incubation, Luc and βgal activities were measured. The Luc activity was presented as relative Luc activity which was normalized based on the G-Luc or βgal activity, or the fold change as compared to the basal reporter level. Representative results of at least three independent biological experiments are shown.

Western blotting

Cells were seeded into a 6-well plate and harvested when they reached 90-100% confluence. The cells were lysed with RIPA buffer containing 1×cOmplete Protease Inhibitor Cocktail (11836153001, Roche). Protein concentrations were determined using a bicinchoninic acid protein assay Kit (5000111, Bio-Rad). Proteins were separated by sodium dodecyl sulfate polyacrylamide gel electrophoresis (SDS-PAGE) and transferred onto 45 μm Polyvinylidene difluoride (PVDF) membrane (IPVH00010, Merck Millipore). Membranes were blocked using 5% skim milk and probed with the respective primary and secondary antibodies. The signal was visualized using Clarity Western ECL Substrate (1705060, Bio-Rad) or exposed to X-ray film (7400, Kodak). The antibodies were raised against the following proteins: phospho-SMAD1/5 (pSMAD1/5, home-made, which recognizes pSMAD1/5, and crossreacts with pSMAD3) [29], phospho-SMAD2 (pSMAD2, home-made) [29], SMAD5 (sc-7443, Santa Cruz), SMAD2 (5339, Cell Signaling Technology), Flag M2 (F3165, Sigma-Aldrich), phospho-ERK1/2 (pERK1/2, 4370, Cell Signaling Technology), ERK1/2 (9102, Cell Signaling Technology), phospho-AKT (pAKT, 9275, Cell Signaling Technology), AKT (9272, Cell Signaling Technology), β-Actin

(A5441, Sigma-Aldrich), glyceraldehyde3-phosphate dehydrogenase (GAPDH, MAB374, Merck Millipore).

Quantitative PCR

Total RNAs were isolated using the NucleoSpin RNA II kit (740955, BIOKE). 1 μg of RNA was reverse transcribed using the RevertAid First Strand cDNA Synthesis Kit (K1621, ThermoFisher Scientific). Quantitative real-time polymerase chain reaction (qRT-PCR) was conducted with GoTaq qPCR Master Mix (A6001, Promega) by CFX Connect Detection System (1855201, Bio-Rad). All target genes expression levels were normalized to *GAPDH*/*Gapdh*. For Droplet Digital PCR (ddPCR), The samples were placed in the Droplet Reader QX200 (Droplet Digital PCR System). The QuantaSoft software determines the absolute starting copy number in units of copies/μl input sample and then reports the target DNA concentration in the form of copies per μl in the sample.

The sequences of primers for detecting target genes are shown as following. Human *ID1*: Forward, CTGCTCTACGACATGAACGG; Reverse, GAAGGTCCCTGATGTAGTCGAT. Human *ID3*: Forward, CACCTCCAGAACGCAGGTGCTG; Reverse, AGGGCGAAGTTGGGGCCCAT. Human *SMAD6*: Forward, ACAAGCCACTGGATCTGTCC; Reverse, ACATGCTGGCGTCTGAGAA. Human *GAPDH*: Forward, TGCACCACCAACTGCTTAGC; Reverse, GGCATGGACTGTGGTCATGAG. Mouse *Id1*: Forward, ACCCTGAACGGCGAGATCA; Reverse, TCGTCGGCTGGAACACAT. Mouse *Id3*: Forward, GCTGAGCTCACTCCGGAACT; Reverse, CGGGTCAGTGGCAAAAGC. Mouse *Gapdh*: Forward, TGGCAAAGTGGAGATTGTTGCC; Reverse, AAGATGGTGATGGGCTTCCCG.

Wound healing assay

MDA-MB-231 (5×10^5 cells/well) were cultured in a 6-well plate and pre-treated with the indicated concentration of TGFβ, BMP7 or FK506 for 24h. Scratches were created using a P200 pipette tip to scratch a straight line on the culture plate through the cell monolayer. The culture medium was replaced with 1% serum fresh medium containing the same treatment as before to remove detached cells. Phase-contrast images were acquired at 0 and 16h post-scratch using a microscope equipped with a CCD camera, and ImageJ was used to analyze the closed area.

Embryonic zebrafish xenograft

All zebrafish experiments were carried out according to the international guidelines and was approved by the local Institutional Committee for Animal Welfare (*Dier Ethische Commissie* (DEC)) of the LUMC. The zebrafish xenograft model was established as described before [24, 30]. Briefly, approximately 400 mCherry-labeled MDA-MB-231 cells were injected into the duct of Curvier (DoC) of transgenic zebrafish embryos (*Fli:enhanced green fluorescent protein (EGFP)*), whose vasculature is marked in green, at 48h post-fertilization. After verification by microscopy, only correctly injected and viable zebrafish were grouped, and received corresponding treatments by directly administrating compounds into egg water. Xenografted zebrafish embryos were maintained at 34°C after injection, a compromise for both the fish and the human cell lines. 5 days post implantation (dpi), the MDA-MB-231 cells that extravasated individually from circulation into the collagen fibers of the tail fin were imaged and counted under a confocal microscope (SP5 STED, Leica Microsystems). All experiments were repeated at least two times independently, and representative experiments are shown.

Whole mount immunostaining of embryonic zebrafish

Embryos at 3dpi were fixed in 4% paraformaldehyde overnight at 4°C. Embryos were permeabilized with 10 μg/ml proteinase K (AM2546, ThermoFisher Scientific), washed, and blocked with phosphate buffered saline (PBS) containing 0.1% triton, 2% goat serum before incubation with pSMAD1/5 (9516, Cell Signaling Technology) overnight at 4°C in 1% goat serum. Secondary antibody Alexa Fluor 350 goat anti-rabbit IgG (Z25300, ThermoFisher Scientific) was used for detection. Embryos were imaged under a confocal microscope (SP5 STED, Leica Microsystems)

Mice experiments

Mice homozygous for the severe combined immune deficiency spontaneous mutation in DNA dependent protein kinase active subunit $Prkdc^{SCID}$ were purchased from animal resource center (ARC, West Australia). All animal experiments were performed in accordance with National Health Medical Research Council of Australia code of practice for the care and use of animals for scientific purposes and approved by The University of Melbourne Animal Ethics Committee (Ethics ID: 1613813).

For BMP signaling restoration model, mice were challenged with 3×10^6 Ad-Bre-Luc labelled MDA-MB-231-G-luc tumor cells (2 tumors/mouse contralaterally) orthotopically into

mammary fat pads at day 0. At 5 dpi, mice were randomly and evenly divided, followed by daily Bioluminescence imaging and treatment via intraperitoneal (i.p.) injection for 5 days. Bioluminescence signal of mice was measured using an in vivo IVIS imaging system (200 Series, Caliper Life Sciences) after being by administrating 150 mg/kg of D-Luciferin (50227, Sigma-Aldrich) via i.p. injection. The signal intensity was analysed using total flux (photons/second) in the regions of interest and normalized to background signal by Living Image software (V3.2, Caliper Life Sciences).

For metastasis model, mice were challenged with 1×10^6 MDA-MB-231 (left side) and 3×10^6 MDA-MB-231-G-luc (right side) tumor cells in the contralateral fat pads at day 0. Mice were randomly and evenly divided at 5 dpi, followed by daily treatment for 3 weeks. Mice were monitored for body weight and tumor size 2-3 times per week. At the endpoint, immediately after sacrifice of the mice, 1ml whole blood each mouse was collected by cardiac puncture and preserved into tube containing heparin. 5µl of the blood samples were lysed and assessed for G-Luc activity, which can represent the degree of circulating tumor cells (CTCs). Blood from mice without MDA-G-LUC tumor implantation was used as a negative control. Unlabeled MDA-MB-231, lung, liver, leg, and brain were harvested for detection of self-seeding and metastasis. Muscle and G-luc labelled tumors were used as negative and positive control, respectively. Three pieces from different sites of all tumors and organs were cut.

Statistics

Data are presented in bar and line graphs as the mean ± standard deviation (s.d) or mean ± standard error (s.e.m) as indicated in the figure legends. All statistical analyses were performed Student's *t* test. $P < 0.05$ indicates statistical significance.

Results

TGFβ abolishes BMP-induced SMAD1/5 activation in highly-invasive breast cancer cells

To determine TGFβ's effect on SMAD1/5 signaling, MDA-MB-231 cells were infected with adenoviral transcriptional reporter Ad-BRE-F-Luc, where the BMP/SMAD1/5 response element drives firefly luciferase expression, and stimulated with TGFβ at different time points. As shown in Figure 1A, SMAD1/5-driven transcription activity was induced by TGFβ initially (up to 6h) Western blotting further confirmed TGFβ's stimulatory and inhibitory effects on SMAD1/5 phosphorylation (Figure 1B). The pSMAD1/5 level was increased in the first 0.5h, then was

reduced to levels lower than the baseline (0h) after 2h. unlike pSMAD1/5, pSMAD3 (downstream of TGFβ type I receptor activation) continued (above baseline) though there was reduction after peaking, indicating a different dynamic response for SMAD3 and SMAD1/5 signaling upon TGFβ stimulation. TGFβ had little effect on Wnt pathway according to Ad-TCF-F-Luc transcriptional reporter assay (Figure S1A), confirming the specificity of TGFβ on inhibition of SMAD1/5 signaling. In fact, TGFβ also suppressed BMP-induced SMAD1/5 phosphorylation in MDA-MB-231 cells. In contrast, this inhibitory effect is much less (Figure 1C) in MCF7 cells, indicating a TGFβ's suppression of BMP-SMAD1/5 signaling is cell context dependent.

To further investigate whether this suppressive effect by TGFβ occurs in cells with different invasiveness, we infected highly-invasive breast basal cancer MDA-MB-231 cell line, non-invasive luminal MCF7 cell line or normal mammary epithelial MCF10A cell line with Ad-Bre-F-Luc and Ad-CAGA-G-Luc for 24h, so that SMAD1/5 and SMAD3 signaling could be quantitated in the same cells at the same time respectively. As shown in Figure 1D, TGFβ suppressed SMAD1/5 signaling significantly and more importantly inhibited BMP-induced SMAD1/5 signaling to the level lower than the basal level (without treatment) in MDA-MB-231 cells. Whereas, in MCF7 cells, the inhibition intensity is not as strong as seen in MDA-MB-231 cells. Notably, TGFβ failed to suppress BMP-induced SMAD1/5 signaling to a level lower than the basal activity in MCF10A cells. Moreover, BMP7 significantly impaired TGFβ signaling activity in these two cell lines, which was not observed in MDA-MB-231 cells. Furthermore, TGFβ-mediated inhibition of SMAD1/5 signaling could be abolished by TGFβ type I receptor inhibitor SB-431542 in a dose-dependent manner (Figure 1E). Taken together, the effectiveness of TGFβ suppressing BMP signaling goes in parallel with the tumor cells' invasiveness.

SMAD6 acts as important negative feedback modulator of the BMP/SMAD signaling pathway [31]. To examine the possibility that TGFβ blocks BMP signaling by inducing SMAD6 expression. We first showed that *SMAD6* mRNA expression increased with TGFβ treatment in MDA-MB-231 cells (Figure S1B). However, only a slightly restoration of TGFβ-inhibited SMAD1/5 signaling could be observed when knockdown *SMAD6* by siRNA(Figure S1C, D). Therefore, we reasoned that SMAD6 may weakly contribute to TGFβ's anti-SMAD1/5 signaling effect but not the main cause.

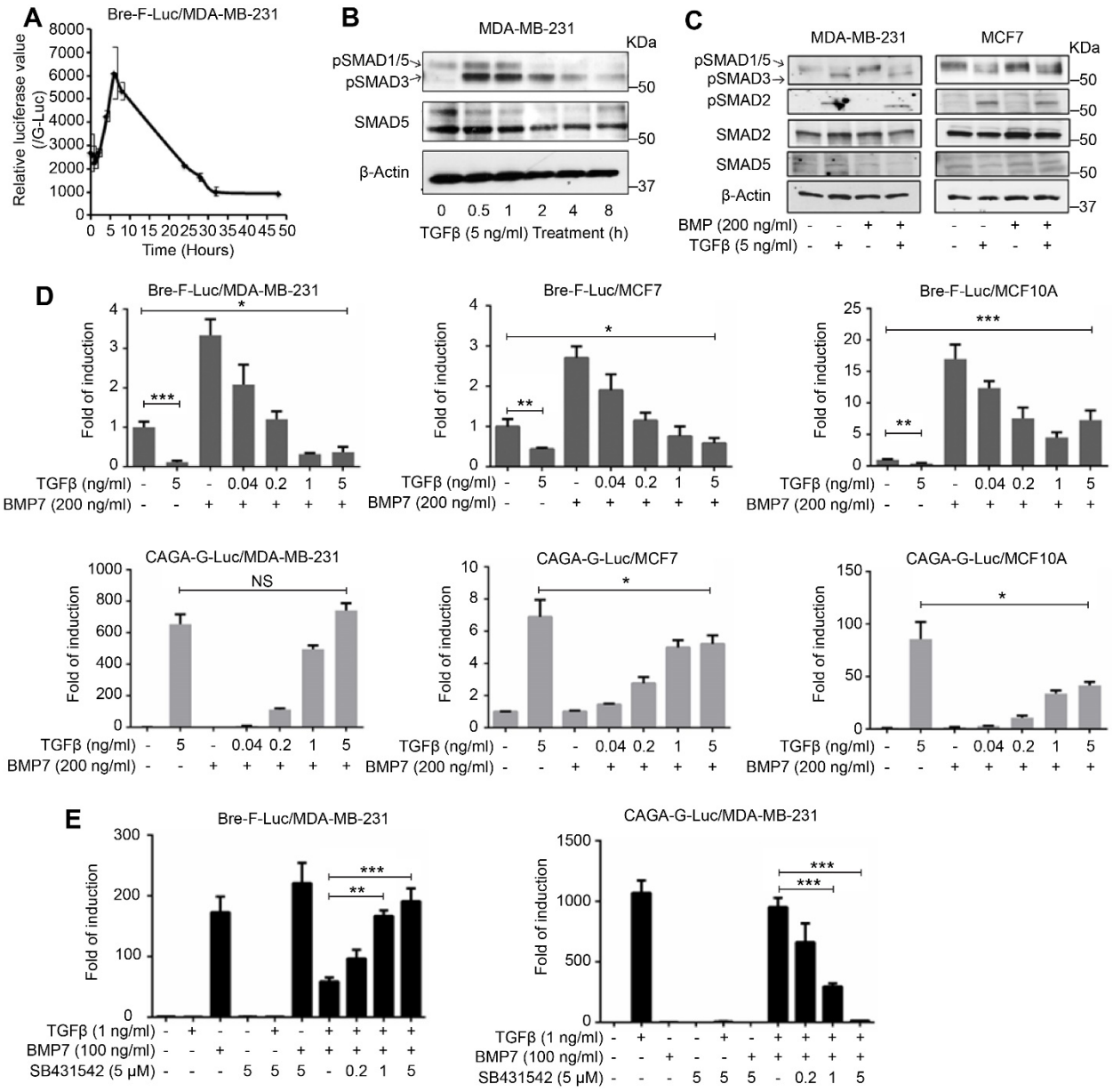

Figure 1. TGFβ impaired BMP signaling activation. A, Kinetic response of BMP signaling reporter (Ad-Bre-F (firefly)-Luc) to TGFβ stimulation (5 ng/ml) in MDA-MB-231 cells. The value is normalized to G (Gaussia)-Luc activity. n = 3. **B**, Kinetic response of SMAD1/5, SMAD3 phosphorylation (pSMAD1/5, pSMAD3, the home-made used here pSMAD1/5 antibody can well cross act with pSMAD3) to TGFβ stimulation (5 ng/ml) in MDA-MB-231 cells. β-Actin is used as a loading control. **C**, TGFβ suppressed BMP-induced SMAD1/5 phosphorylation (pSMAD1/5) in MDA-MB-231 cells, not in MCF7 cells. β-Actin is used as a loading control. **D**, BMP/TGFβ-SMAD signaling reporter (Ad-Bre-F-Luc/Ad-CAGA-G-Luc) assay in response to BMP/TGFβ alone or combination stimulation in MDA-MB-231, or MCF7, or MCF10A cells. The results are expressed as the mean ± s.d, n = 3. Student's *t* test, NS, not

significant, *$P < 0.05$, ***$P \leq 0.001$. **E**, Impaired response of BMP/SMAD signaling reporter (Ad-Bre-F-Luc) to BMP stimulation by TGFβ is restored by TGFβ type I receptor inhibitor SB431543 in MDA-MB-231 cells. The value is normalized to G-Luc activity. The results are expressed as the mean ± s.d, n = 3. Student's *t* test, **$P \leq 0.01$, ***$P \leq 0.001$.

MEK inhibitors specifically restore BMP signaling activity

To further explore other possible mechanism of TGFβ suppression of SMAD1/5 signaling, we resorted to non-canonical TGFβ signaling [19, 20]. Surprisingly, TGFβ-induced prolonged ERK1/2 phosphorylation in MDA-MB-231 cells as shown in Figure 2A. TGFβ also induced transient AKT phosphorylation suggesting temporary activation of PI3K signaling. Next, two selective small molecule MEK inhibitors (U0126 and PD98059) and PI3K inhibitor (LY294002) were utilized to investigate whether these pathways are involved in TGFβ-induced inhibition of SMAD1/5 signaling in MDA-MB-231 cells. As shown in Figure 2B, U0126 or PD98059 treatment significantly enhanced BMP/SMAD1/5-dependent transcription activity, and overcame TGFβ mediated inhibitory effect on SMAD1/5 signaling. However, LY294002 treatment had little effect on SMAD1/5 signaling (Figure 2C). Perturbation of TGFβ's activation of AKT and ERK1/2 had no effect on TGFβ-SMAD3-dependent transcriptional reporter activity (Figure 2B, C).

For further conformation, we manipulated MAPK/ERK pathway activation independent of TGFβ. In A431 and HN5 cells lines, where the EGF receptor (EGFR) is highly expressed [32], EGF stimulation significantly suppressed BMP-induced SMAD1/5 activation. Importantly, U0126 treatment ameliorated such suppression (Figure 2D). Additionally, BMP-induced SMAD1/5 activation in Ras-transformed 21D1 cells was significantly lower than in its parental MDCK cells. TGFβ-induced inhibition of SMAD1/5 activity in 21D1 cells could be fully restored by U0126 (Figure 2E). Furthermore, using a doxycycline-inducible-Ras expression NIH3T3 fibroblasts (Figure 2F), similar results were obtained, except U0126 further amplified BMP-SMAD1/5 signaling in inducible NIH3T3 fibroblasts without doxycycline treatment, possibly due to leaky Ras expression in this system [23]. Collectively, these data established that MAPK/ERK activation abolishes BMP-SMAD1/5 activation, which could be reversed by small molecule MEK inhibitors.

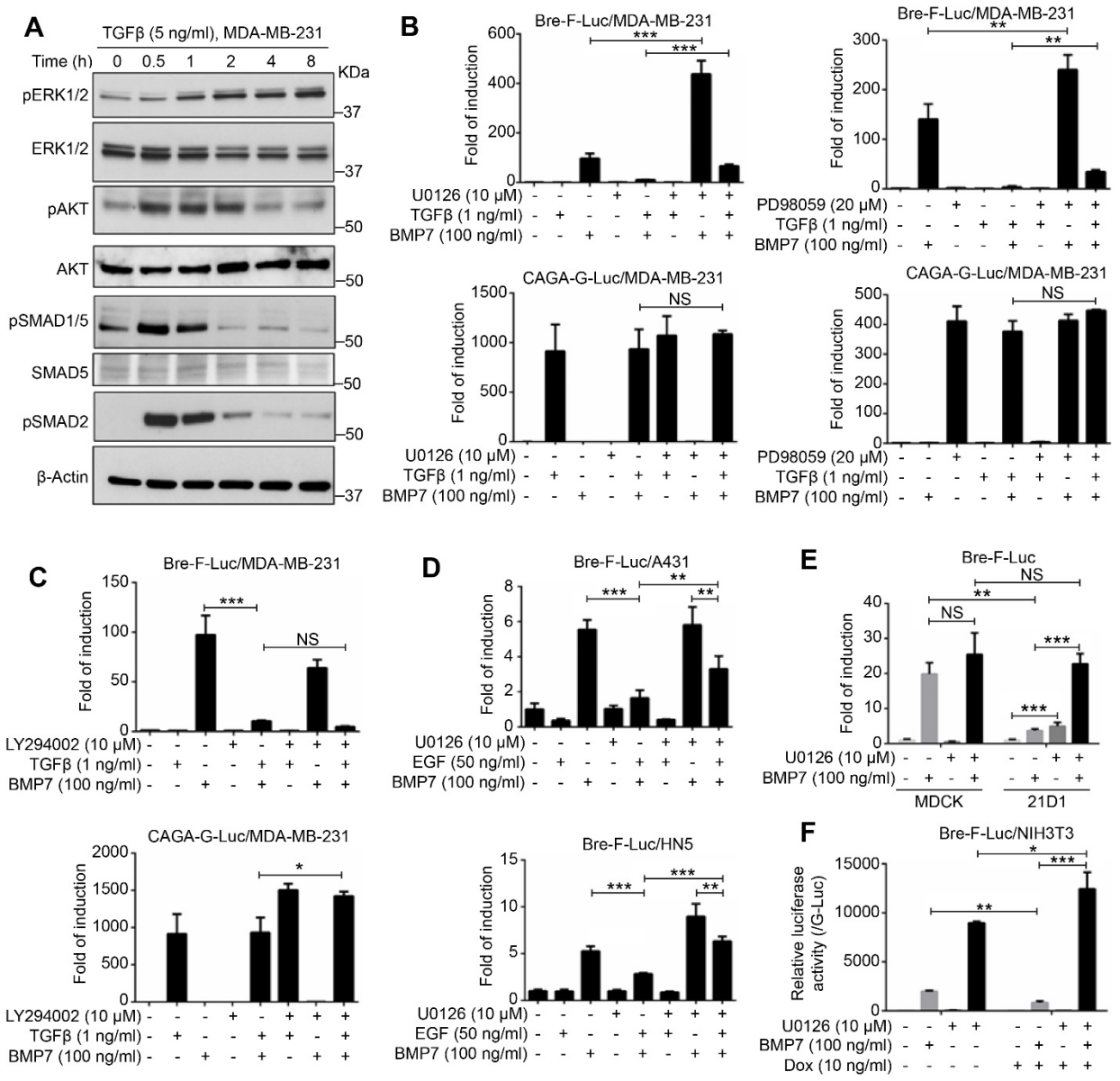

Figure 2. Prolonged ERK1/2 activation induced by TGFβ mediated inhibition of BMP signaling. A, TGFβ induced sustained ERK1/2 activation in MDA-MB-231 cells. The level of ERK1/2, SMAD1/5, SMAD2 phosphorylation (pERK1/2, pSMAD1/5, pSMAD2), ERK1/2, SMAD1/5, were determined by western blotting. β-Actin is used as a loading control. **B**, TGFβ-inhibited SMAD1/5 signaling (Ad-Bre-F (firefly)-Luc assay) could be restored by administration of MEK inhibitors, U0126 or PD98059, in MDA-MB-231 cells. SMAD3 signaling (Ad-Bre-G (Gaussia)-Luc assay) is not affected. **C**, PI3K inhibitor LY294002 could not interfere the inhibition of TGFβ on SMAD1/5 signaling (Ad-Bre-F-Luc assay) in MDA-MB-231 cells. SMAD3 signaling (Ad-Bre-G-Luc assay) is not affected. The results are expressed as the mean ± s.d, n = 3. Student's *t* test, NS, not significant, $*P \leq 0.05$, $***P \leq 0.001$. **D**, U0126 restores EGF-inhibited SMAD1/5 signaling (Ad-Bre-F-Luc assay) in EGFR redundant cell lines, A431 and HN5.

The results are expressed as the mean ± s.d, n = 3. Student's *t* test, $^{**}P \leq 0.01$, $^{***}P \leq 0.001$. **E**, U0126 restores SMAD1/5 signaling (Ad-Bre-F-Luc assay) inhibited by sustain activation of MAPK/ERK in 21D1 cells, which is derived from H-Ras transformed MDCK cells. The results are expressed as the mean ± s.d, n = 3. Student's *t* test, NS, not significant, $^{**}P \leq 0.01$, $^{***}P \leq 0.001$. **F**, U0126 restores SMAD1/5 signaling (Ad-Bre-F-Luc assay) inhibited by induced activation of MAPK/ERK in doxycycline-inducible-Ras transformed NIH3T3 cells. The results are expressed as the mean ± s.d, n = 3. Student's *t* test, $^{*}P < 0.05$, $^{**}P \leq 0.01$, $^{***}P \leq 0.001$.

FK506 is a selective BMP-SMAD1/5 agonist in breast cancer cells

We screened for small molecule compounds that can work as a BMP-SMAD1/5 signaling agonist by testing a panel of FDA approved drugs and biologically active compounds for ability

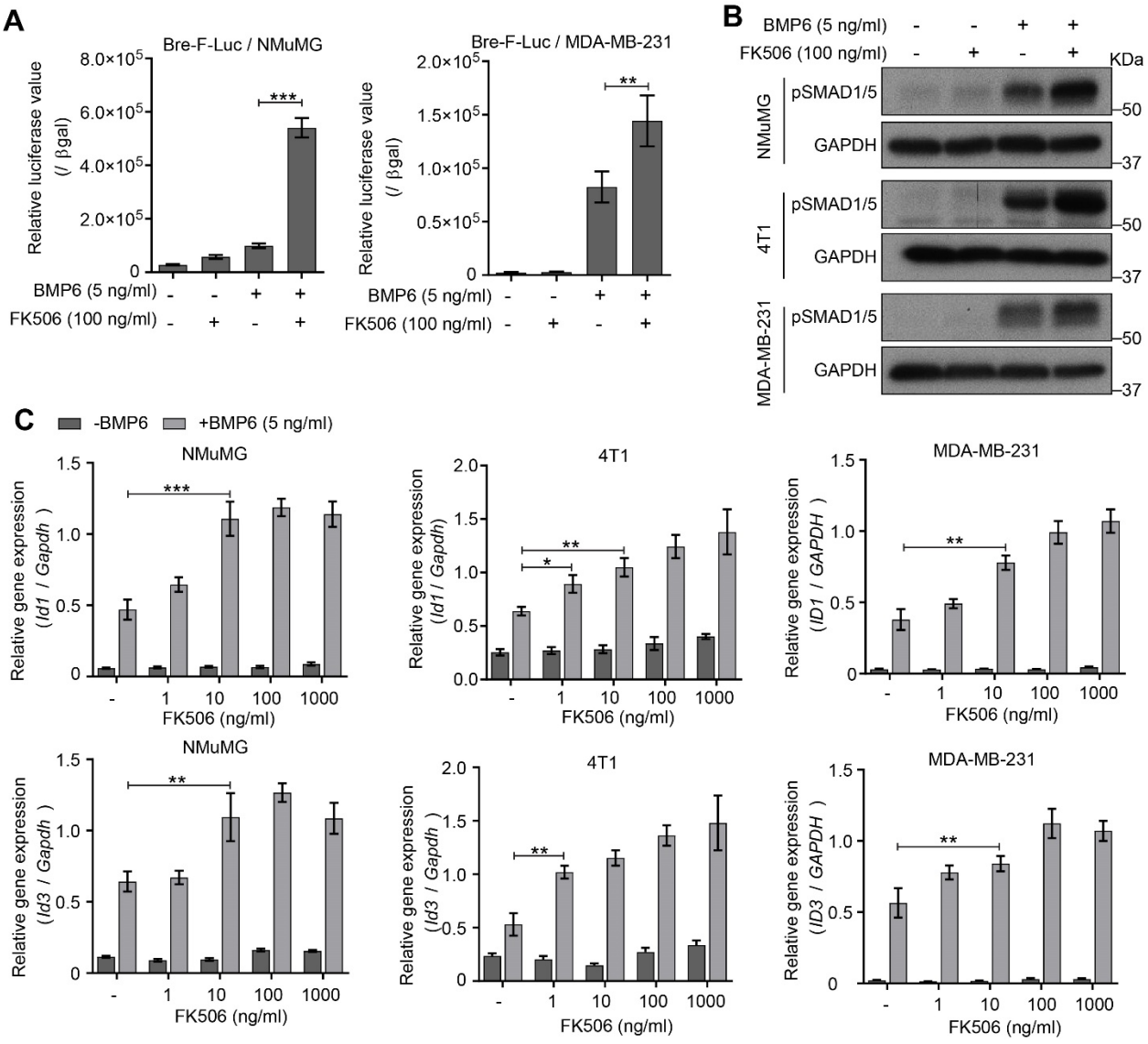

Figure 3. FK506 activates BMP signaling, but not TGFβ signaling. A, FK506 enhances BMP signaling by Bre-F (firefly)-Luc reporter assay in NMuMG or MDA-MB-231 cells. The value is normalized to βgal activity. The results are expressed as the mean ± s.d, n = 3. Student's *t* test, $^{**}P \leq 0.01$, $^{***}P \leq 0.001$. **B**, FK506 promotes BMP-mediated SMAD1/5 phosphorylation (pSMAD1/5) by western blotting in NMuMG, or 4T1, or MDA-MB-231 cells. GAPDH is used as a loading control. **C**, FK506 promotes expression of BMP signaling target genes, *Id1*/*3* in NMuMG, or 4T1 cells, *ID1*/*3* in MDA-MB-231 cells. *Gapdh* or *GAPDH* is used as an internal control. The results are expressed as the mean ± s.d, n = 3. Student's *t* test, $^{*}P < 0.05$, $^{**}P \leq 0.01$, $^{***}P \leq 0.001$.

to activate Bre-Luc transcriptional reporter activity in breast NMuMG cells (Figure S3A). The result showed that FK506 (Tacrolimus) is the most potent activator among tested compounds. Indeed, previous study had shown that FK506 can activate BMP signaling in endothelial cells by interfering with binding of negative regulator FKBP12 to BMP type I receptors [33]. We found that FK506 strongly promoted BMP signaling, as shown by increased Bre-Luc reporter activity (Figure 3A), SMAD1/5 phosphorylation (Figure 3B), and BMP/SMAD1/5 target genes (*ID1*/*3*) expression (Figure 3C) in several tested breast cell lines, NMuMG, 4T1, MDA-MB-231. FK506-mediated promotion of SMAD1/5 phosphorylation could be blocked by addition of a selective BMP type I receptor kinase inhibitor LDN193189 to cells (Figure S3B). We observed that the TGFβ-SMAD3 pathway was not affected by FK506 treatment (Figure S3C, D, E). This was contrary what we expected as FKBP12 has been previously reported to bind to all TGFβ family type I receptors [34]. Instead, we found that FK506 treatment slightly but significantly inhibited TGFβ-SMAD3 signaling in NMuMG cells (Figure S3C, D, E). What's more, FK506 treatment had little effect on TGFβ-induced phosphorylation of ERK1/2 in MDA-MB-231 cells (Figure S3F).

The combination of suboptimal dosages of U0126 and FK506 treatment exhibits synergistic effect on BMP signaling restoration *in vitro*

Given that U0126, PD98059 and FK506 were able to restore BMP signaling at 10μM, 20μM and 100ng/ml, respectively, this may raise a potential risk of side effects on clinical usage. Therefore, we questioned if lower concentration of U0126, or PD98059 or FK506 could synergistically amplify BMP signaling. Cells were incubated with various doses of these drugs in the presence of BMP. As a result, the fold of induction increased with U0126, PD98059 and FK506 treatment in a dose-dependent manner. Even 1μM U0126, 4ng/ml FK506 and 2μM PD98059 was able to

enhance SMAD1/5 signaling significantly (Figure 4A). Herein, we tried to combine U0126 and FK506 at their suboptimal concentrations to minimize the potential toxicity. As expected, combination of 1μM U0126 and 20ng/ml FK506 amplified BMP-induced SMAD1/5 signaling synergistically. Meanwhile, the combination treatment exhibited synergistic effect on restoration of SMAD1/5 signaling in the presence of TGFβ, to extent of higher than BMP single treatment. Again, TGFβ-SMAD3 signaling was not influenced by U0126 or/and FK506 stimulation (Figure 4B) in the very same cells where BMP/SMAD1/5 signaling were enhanced.

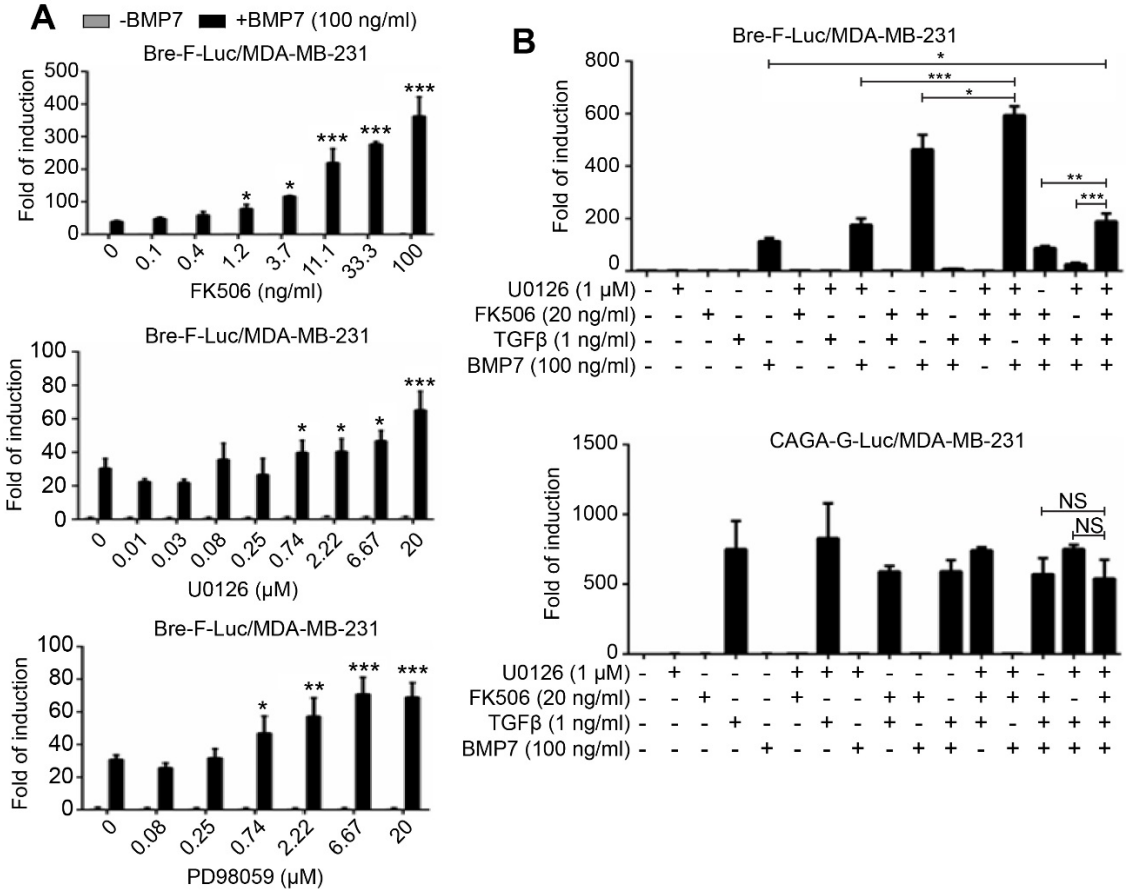

Figure 4. The combination treatment of suboptimal concentration of U0126 and FK506 exhibits synergistic effect on amplification of BMP signaling. A, FK506, or U0126, or PD98059 could restore SMAD1/5 signaling (Ad-Bre-F (firefly)-Luc assay) at low dose in MDA-MB-231 cells. The results are expressed as the mean ± s.d, n = 3. Student's *t* test, **P* <0.05, ***P* ≤ 0.01, ****P* ≤ 0.001. **B**, U0126 and FK506 combination at suboptimal dose shows synergistic effect on amplification of BMP signaling (Ad-Bre-F-Luc assay) in MDA-MB-231 cells. SMAD3signaling (Ad-CAGA-G (Gaussia)-Luc assay) is not affected. The results are expressed as the mean ± s.d, n = 3. Student's *t* test, NS, not significant, **P* < 0.05, ***P* ≤ 0.01, ****P* ≤ 0.001.

Combination treatment of suboptimal FK506 and U0126 suppresses MDA-MB-231 cells metastasis in zebrafish xenograft model

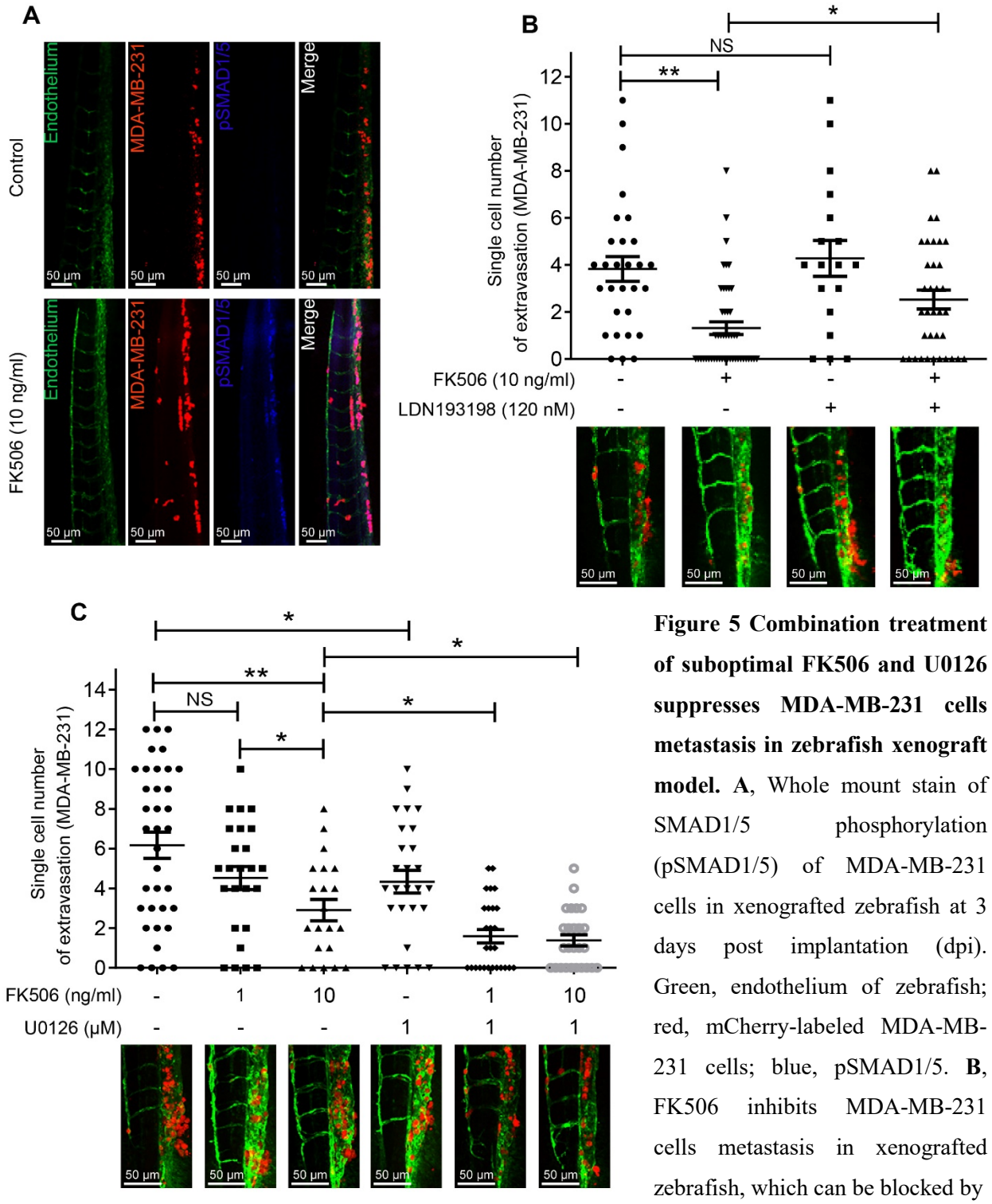

Figure 5 Combination treatment of suboptimal FK506 and U0126 suppresses MDA-MB-231 cells metastasis in zebrafish xenograft model. A, Whole mount stain of SMAD1/5 phosphorylation (pSMAD1/5) of MDA-MB-231 cells in xenografted zebrafish at 3 days post implantation (dpi). Green, endothelium of zebrafish; red, mCherry-labeled MDA-MB-231 cells; blue, pSMAD1/5. **B**, FK506 inhibits MDA-MB-231 cells metastasis in xenografted zebrafish, which can be blocked by LDN193189. The graph shows the quantification of the number of intravasated cells in each embryonic body at 5dpi. The results are expressed as the mean ± s.e.m, n = 2. Student's t test, NS, not significant, *P

< 0.05, **$P \leq 0.01$. The panel shows the representative images. Green, *Fli*:*EGFP* labelled endothelium of zebrafish; red, mCherry-labeled MDA-MB-231 cells. **C**, Combination treatment of suboptimal FK506 and U0126 on MDA-MB-231 cells extravasation in xenografted zebrafish. The graph, panel description and statistical analysis are the same as described in **B**.

We wondered if enhanced BMP signaling functionally affects cancer cell migration *in vitro*. As shown in Figure S3A, FK506 treatment of MDA-MB-231 cells failed to suppress cell migration in wound healing assay. Using zebrafish xenograft model, mCherry labelled MDA-MB-231 cells were injected into zebrafish blood stream. Then zebrafish were subjected to FK506 treatment. Clearly activation of BMP signaling in MDA-MB-231 cells in xenografted zebrafish and in host zebrafish cells could be observed by whole mount immunostaining of pSMAD1/5 at 3dpi upon treatment with FK506 (Figure 5A). At 5dpi, the result showed FK506 decreased number of extravasated cells in the tail fin of zebrafish in a dose dependent manner (Figure S3B). Moreover, BMP type I receptor inhibitor LDN193189 reversed FK506-mediated inhibition of MDA-MB-231 cells metastasis (Figure 5B). These results suggest that activation of SMAD1/5 signaling in MDA-MB-231 and/or zebrafish host cells inhibits extravasation of these cells.

In view of U0126 and FK506 synergistically enhanced BMP signaling *in vitro*, xenografted zebrafish were challenged with combinational treatment to investigate if synergistic inhibition of breast cancer metastasis could be achieved. The result showed that U0126 and FK506 combination at suboptimal dose treatment led to dramatic inhibition of MDA-MB-231 cells metastasis. The number of extravasated cells was reduced by single U0126 treatment. This is probably due to the involvement of MAPK/ERK pathway in regulating cell migration [35].When looking at the detail, 1 ng/ml FK506 treatment did not inhibit cancer cell metastasis significantly, whereas combining such low dose of FK506 (1 ng/ml) with U0126 displayed significant inhibition effect on MDA-MB-231 cell extravasation (Figure 5C).

FK506 and U0126 treatments suppress tumor self-seeding, liver and bone metastasis in mice model

Then, we sought to study synergistic effect of U0126 and FK506 alone or in combination on metastasis of MDA-MB-231 cells in mice model. G-Luc labelled MDA-MB-231 cells were infected with Ad-Bre-F-Luc reporter and then implanted orthotopically in the mammary fat pads of mice to monitor BMP signaling activation by IVIS imaging (Figure 6A). Mice were imaged and treated daily at 5dpi. The treatment dosages in mice were equivalent to the suboptimal

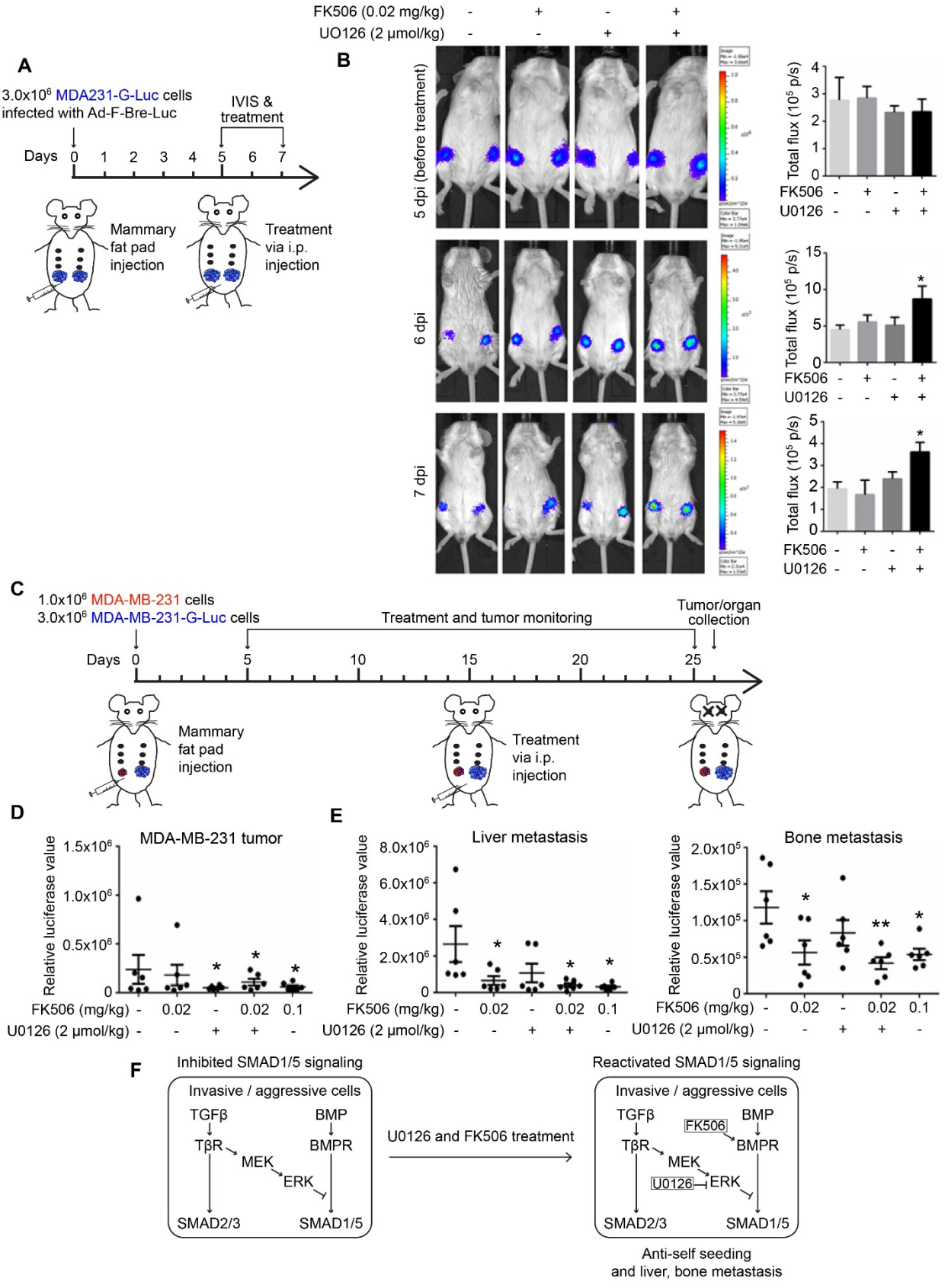
A
3.0x10⁶ MDA231-G-Luc cells
infected with Ad-F-Bre-Luc
IVIS & treatment
Days 0 1 2 3 4 5 6 7
Mammary fat pad injection
Treatment via i.p. injection
B
FK506 (0.02 mg/kg) - + - +
UO126 (2 μmol/kg) - - + +
5 dpi (before treatment)
6 dpi
7 dpi
Total flux (10⁵ p/s)
FK506 - + - +
U0126 - - + +
C
1.0x10⁶ MDA-MB-231 cells
3.0x10⁶ MDA-MB-231-G-Luc cells
Treatment and tumor monitoring
Tumor/organ collection
Days 0 5 10 15 20 25
Mammary fat pad injection
Treatment via i.p. injection
D
MDA-MB-231 tumor
Relative luciferase value
FK506 (mg/kg) - 0.02 - 0.02 0.1
U0126 (2 μmol/kg) - - + + -
E
Liver metastasis
Bone metastasis
F
Inhibited SMAD1/5 signaling
Invasive / aggressive cells
TGFβ
BMP
TβR
BMPR
MEK
ERK
SMAD2/3
SMAD1/5
U0126 and FK506 treatment
Reactivated SMAD1/5 signaling
FK506
U0126
Anti-self seeding and liver, bone metastasis

Figure 6. Combination treatment of FK506 and U0126 suppresses tumor self-seeding, liver and bone metastasis in mice. A, A diagram of BMP signaling detection experiment. MDA-MB-231-G (Gaussia)-Luc cells were infected with Ad-Bre-F-Luc two days before tumor implantation. $3x10^6$ cells were orthotopically injected into the mammary fat pads of immunocompromised SCID mice (2 tumors/mouse contralaterally, 3 mice/group). Daily treatments started at day 5. 24h later, the reporter activity in the tumors was measured by IVIS Lumina imaging system following intraperitoneal (i.p.) injection with 150mg/kg D-Luciferin. **B**, Representative figures (left) and corresponding quantification of the signal in the mammary fat pad area (right) at 5 days post implantation (dpi, before treatment), 6dpi, 7dpi. The results are expressed as the mean ± s.e.m., Student's t test, $*P < 0.05$, **C**, A diagram of breast cancer metastasis experiment. MDA-MB-231 and MDA-MB-231-G-Luc cells were orthotopically injected into mammary fat pads of SCID mice (2 tumors/mouse contralaterally, 6 mice/group) as shown. Daily treatment started at 5 dpi through i.p. injection. 3 weeks later, mice were sacrificed for tumor/organ collection. **D**, **E**, Unlabeled tumor (MDA-MB-231), liver and bone were lysed to determining G-Luc activity. The results are expressed as the mean ± s.e.m, Student's *t* test, $*P < 0.05$, $**P \leq 0.01$. **F**, Working model. In normal cells, TGFβ-SMAD2/3 signaling could not interfere BMP-SMAD1/5 signaling evidently. In invasive/aggressive cells, TGFβ inhibits SMAD1/5 signaling via activation of MAPK/ERK pathway. Enhancing BMP-SMAD1/5 signaling by U0126 and FK506 combination treatment reduces cancer cell metastasis.

dosages *in vitro*. 24, 48h after (6, 7dpi), bioluminescent signals in U0126 and FK506 combination treated mice were higher than that in control, while single treatment of U0126 or FK506 had little effect on BMP-SMAD1/5 signaling. This result indicates efficient BMP signaling activation by the combination of suboptimal dosages of these two drugs *in vivo* (Figure 6B).

Next, mice were challenged with MDA-MB-231 and MDA-MB-231-G-Luc tumor cells in contralateral mammary fat pads respectively. Five days later, mice were treated as indicated and monitored for another three weeks (Figure 6C). U0126 or/and FK506 treatment had little effect on primary tumor growth (Figure S4A). Circulating tumor cells (CTCs) were analyzed by measuring the G-Luc activity of lysed blood sample. Interestingly, as shown in Figure S4B, CTCs number in different treatment groups were almost the same. We reasoned that the shedding of tumor cells into the circulation was mainly TGFβ-regulated, which was not influenced by U0126/FK506 stimulation as indicated *in vitro*. Previously, CTCs were reported to re-infiltrate an established tumor, in a process termed "tumor self-seeding" [36]. MDA-MB-231

tumors were collected and lysed for detecting tumor self-seeding. The result indicated that U0126, U0126/FK506 combination and higher dose of FK506 treatments significantly reduced MDA-MB-231-G-Luc tumor cells self-seeding. This indicates BMP signaling efficiently suppressed tumor cells colonizing their tumors of origin. Lower dose of FK506 decreased tumor cell self-seeding as well but it was not statistically significant (Figure 6D). In addition, G-Luc activity in mice liver, lung, bone and brain were measured for evaluating intensity of cancer cell metastasis. Both liver and bone metastasis were reduced by low or high dose of FK506 compared to control group. Combination treatment of FK506 and U0126 at low dose further inhibited metastasis compared to low dose of FK506 treatment, even there is no significant difference. U0126 alone did not decrease liver and bone metastasis significantly (Figure 6E). The aforementioned treatments did not lead to significant reduction in lung and brain metastasis (Figure S4C), suggesting that restored BMP signaling plays a differential role in organ specific metastasis. Taken together, enhancement of BMP signaling activity *in vivo* by FK506 and U0126 treatment efficiently suppressed tumor self-seeding and distant organ metastasis especially to liver and bone (Figure 6F).

Discussion

In the present study we found that BMP-SMAD1/5 signaling could be abolished by TGFβ in highly metastatic MDA-MB-231 cells, but to a lesser extent in non-invasive MCF7 cells and even weaker inhibitory effect in normal mammary epithelial MCF10A cell. Importantly, chemical activation of BMP-SMAD1/5 signaling inhibited extravasation and metastasis of breast cancer cells. Thus, the TGFβ stimulatory effect on the invasion and metastasis of breast cancer cells is not only induced by directly activating SMAD2/3 as reported [2, 3], progressive loss or suppression of BMP-SMAD1/5 signaling by TGFβ could be an important factor for metastatic cancer development (Figure 6F).

The underlying mechanism by TGFβ inhibits SMAD1/5 activation relates to the its sustained activation of MAPK/ERK in aggressive MDA-MB-231 cells. Challenging of MDA-MB-231 cells with MEK inhibitors, resulted in a reactivation of SMAD1/5 signaling. Consistent with these finding we found that EGF-induced overactivation of MEK in A431 and HN5 cells that express high EGF receptor or activation of MEK by inducible overexpression of active Ras in NIH3T3 fibroblasts elicited a strong inhibition of BMP-SMAD1/5 signaling. Previously, multiple studies have reported BMP signaling and TGFβ signaling can antagonize mutually in

physiological process, like tissue morphogenesis and organogenesis, and also in pathological setting, mainly fibrotic and cancerous diseases [5, 37]. This antagonism was reported to occur at the level of common mediator SMAD4 by competing with limiting amounts for this common mediator [17], MAPK/ERK inducing SMAD1/5 phosphorylation in linker region leading a SMAD1/5 cytoplasmic retention [38], by formation of SMAD1/5-SMAD2/3 mixed complexes [39], or by antagonism by a TGFβ-induced target genes [40]. All these mechanisms occur downstream of pSMAD1/5, whereas we found that MEK pathway activation inhibits upstream of pSMAD1/5. TGFβ-induction of inhibitory SMAD6 that could inhibit BMP-SMAD1/5 response, was found to play, if any, a minor role. Another possibility could be that MEK activation induces an activation of a phosphatase that triggers pSMAD1/5 dephosphorylation. Genetic screening efforts suggest a role for PPM1A phosphatase, which is under current investigation.

In parallel, we identified FK506 as an agonist of BMP-SMAD1/5 signaling in breast cancer cells. This finding is consistent with previous reports in which FK506 is shown to displace the negative regulator FKBP12 from BMP type I receptors [33]. It is not clear to us why FK506 did not activate TGFβ-SMAD2/3 signaling in breast cancer cells as FKBP12 has been reported to interact with all TGFβ family type I receptors [34]. A possibility is that FK506 has other interaction partners that negatively regulate pSMAD1/5. Multiple FK506 interaction partners have peptidyl-prolyl cis/trans isomerase activity, of which activity is inhibited by FK506 [41]. Peptidyl-prolyl cis/trans isomerase Pin1 was found to stabilize SMAD1 and promote BMP-SMAD1/5 signaling [42]. The slight inhibitory effect of FK506 that we observe may have been caused by the increased BMP-SMAD1/5 signaling antagonizing TGFβ-SMAD3 signaling.

Consistent with notion that BMP-SMAD1/5 signaling has a tumor suppressive effect we found that a single dose of MEK inhibitor U0126 or FK506 alone inhibited breast cancer cell extravasation and metastasis. The FK506-induced inhibition of breast cancer cell extravasation was blocked by treatment with BMP type I receptor kinase inhibitor. This is consistent with the action of FK506 promoting BMP type I receptor kinase activity [33]. Of note, a low-dose FK506 was previously shown to activate BMP signaling and inhibit bladder cancer progression [43].

Importantly, we demonstrated a synergistic effect arose in restoring BMP signaling *in vitro*/*vivo* by combining U0126 and FK506 at suboptimal concentrations. Combination treatment by both small molecules synergistically suppressed breast cancer cells extravasation in zebrafish xenograft model and self-seeding and adaptation to distant organs to liver and bone in mice

(Figure 6F). This could be beneficial to patients who may suffer from high dose drug side effects. FK506 is being used as an immunosuppressant to prevent the rejection of organ transplants. Applying FK506 on cancer patient could weaken the host anti-tumor immunity. Even a good treatment response to anti-PD1 immunotherapy was reported in an advanced urothelial carcinoma patient with kidney transplant who received simultaneously FK506 treatment [44]. Recently, a FK506 analog FKVP without immunosuppressive activity was developed to enhance BMP-SMAD1/5 signaling [23]. We found that FKVP potently activated BMP/SMAD1/5 signaling in mammary epithelial NMuMG cells (Figure S5). Thus, FKVP could be explored as a potential FK506 substitute in treatment of cancer metastasis. For MEK inhibitor, several inhibitors have been approved by FDA, and could be tested as an alternative for U0126.

While U0126 and FK506 co-treatment achieved a strong inhibition of metastasis to liver and bone, no effect was observed for lung and brain metastasis. This suggests that the chemical reactivation of BMP signaling has a differential organ effect on breast cancer homing/reseeding. Different organs likely have different TGFβ and BMP bioavailability and thereby influence breast cancer metastasis behavior, and ability of FK506 and U0126 combination to inhibit metastasis. It is a possibility that U0126 and/or FK506 do not reach each organ equally efficient. For example, both compounds may not pass the blood brain barrier efficiently and therefore no effect on brain metastasis by combination treatment was observed.

In conclusion, even though more detailed future studies are required, especially in a clinical setting, before clinical application of our observations can be initiated. Our study provides the feasibility that synergistic activation of BMP signaling by two small molecules at suboptimal dose can achieve a robust decrease in breast cancer metastasis.

Acknowledgements

This study was supported by Cancer Genomics Centre.NL (CGC.NL to PtD) and Chinese Scholarship Council (to JR). We thank Prof. Dr. Paschalis Sideras (Biomedical Research Foundation, Academy of Athens) for valuable discussions, and Maarten van Dinther and Midory Thorikay for technical assistance. We are grateful to Dr. A. Hinck and S. Vukicevic for gift of recombinant ligands and FKVP was kindly provided by Prof. Dr. Jun O. Liu (Johns Hopkins School of Medicine).

Author contributions

PtD and HZ designed and supervised the study. JR and YW conceived experiments and analyzed the majority of the data. JR YW, and JI performed the majority of experiments. JR and YW

prepared the figures, drafted, and wrote the manuscript, which was substantially proof-read, commented, and edited by all authors.

Conflicts of Interest

None of authors has conflict of interest.

Reference

1. Obenauf AC, Massagué J. Surviving at a distance: Organ-specific metastasis. Trends in Cancer 2015;1:76-91.
2. Tsubakihara Y, Moustakas A. Epithelial-mesenchymal transition and metastasis under the control of transforming growth factor β. Int J Mol Sci 2018;19:3672.
3. Derynck R, Muthusamy BP, Saeteurn KY. Signaling pathway cooperation in TGFβ-induced epithelial–mesenchymal transition. Curr Opin Cell Biol 2014;31:56-66.
4. Ren J, ten Dijke P. Bone Morphogenetic Proteins in the Initiation and Progression of Breast Cancer. Bone Morphogenetic Proteins: Systems Biology Regulators, Springer 2017, p.409-33.
5. Wakefield LM, Hill CS. Beyond TGFβ: roles of other TGFβ superfamily members in cancer. Nat Rev Cancer 2013;13:328-41.
6. Scheel C, Eaton EN, Li SH-J, Chaffer CL, Reinhardt F, Kah KJ, *et al*. Paracrine and autocrine signals induce and maintain mesenchymal and stem cell states in the breast. Cell 2011;145:926-40.
7. Ehnert S, Zhao J, Pscherer S, Freude T, Dooley S, Kolk A, *et al*. Transforming growth factor β1 inhibits bone morphogenic protein (BMP)-2 and BMP-7 signaling via upregulation of Ski-related novel protein N (SnoN): possible mechanism for the failure of BMP therapy? BMC Med 2012;10:101.
8. Gao H, Chakraborty G, Lee-Lim AP, Mo Q, Decker M, Vonica A, *et al*. The BMP inhibitor Coco reactivates breast cancer cells at lung metastatic sites. Cell 2012;150:764-79.
9. Ren J, Smid M, Iaria J, Salvatori DC, van Dam H, Zhu HJ, *et al*. Cancer-associated fibroblast-derived Gremlin 1 promotes breast cancer progression. Breast Cancer Res 2019;21:1-19.
10. Eckhardt BL, Cao Y, Redfern AD, Chi LH, Burrows AD, Roslan S, *et al*. Activation of canonical BMP4-SMAD7 signaling suppresses breast cancer metastasis. Cancer Res 2020:canres.0743.2019.
11. Buijs JT, Henriquez NV, van Overveld PG, van der Horst G, Que I, Schwaninger R, *et al*. Bone morphogenetic protein 7 in the development and treatment of bone metastases from breast cancer. Cancer Res 2007;67:8742-51.

12. Naber HP, Wiercinska E, Pardali E, van Laar T, Nirmala E, Sundqvist A, *et al*. BMP-7 inhibits TGFβ-induced invasion of breast cancer cells through inhibition of integrin β3 expression. Cell Oncol 2012;35:19-28.
13. Shi Y, Massagué J. Mechanisms of TGFβ signaling from cell membrane to the nucleus. Cell 2003;113:685-700.
14. Derynck R, Budi EH. Specificity, versatility, and control of TGFβ family signaling. Sci Signal 2019;12:eaav5183.
15. Heldin CH, Moustakas A. Signaling receptors for TGFβ family members. 2016;8:a022053.
16. Furtado MB, Solloway MJ, Jones VJ, Costa MW, Biben C, Wolstein O, *et al*. BMP/SMAD1 signaling sets a threshold for the left/right pathway in lateral plate mesoderm and limits availability of SMAD4. Genes Dev 2008;22:3037-49.
17. Candia AF, Watabe T, Hawley SH, Onichtchouk D, Zhang Y, Derynck R, *et al*. Cellular interpretation of multiple TGFβ signals: intracellular antagonism between activin/BVg1 and BMP-2/4 signaling mediated by Smads. Development 1997;124:4467-80.
18. Gronroos E, Kingston IJ, Ramachandran A, Randall RA, Vizan P, Hill CS. Transforming growth factor β inhibits bone morphogenetic protein-induced transcription through novel phosphorylated Smad1/5-Smad3 complexes. Mol Cell Biol 2012;32:2904-16.
19. Zhang YE. Non-Smad signaling pathways of the TGFβ family. Cold Spring Harb Perspect Biol 2017;9:a022129.
20. Mu Y, Gudey SK, Landström MJ. Non-Smad signaling pathways. Cell Tissue Res 2012;347:11-20.
21. Javelaud D, Mauviel A. Crosstalk mechanisms between the mitogen-activated protein kinase pathways and Smad signaling downstream of TGFβ: implications for carcinogenesis. Oncogene 2005;24:5742.
22. Liu S, Iaria J, Simpson RJ, Zhu HJ, Signaling. Ras enhances TGFβ signaling by decreasing cellular protein levels of its type II receptor negative regulator SPSB1. Cell Commun Signal 2018;16:10.
23. Hoppe PS, Coutu DL, Schroeder T. Single-cell technologies sharpen up mammalian stem cell research. Nat Cell Biol 2014;16:919-27.
24. Ren J, Liu S, Cui C, ten Dijke P. Invasive Behavior of Human Breast Cancer Cells in Embryonic Zebrafish. J Vis Exp 2017;122:e55459.
25. Miller FR, Soule HD, Tait L, Pauley RJ, Wolman SR, Dawson PJ, *et al*. Xenograft model of progressive human proliferative breast disease. J Natl Cancer Inst 1993;85:1725-32.
26. Cuny GD, Paul BY, Laha JK, Xing X, Liu JF, Lai CS, *et al*. Structure–activity relationship study of bone morphogenetic protein (BMP) signaling inhibitors. Bioorg Med Chem Lett 2008;18:4388-92.

27. Luwor RB, Hakmana D, Iaria J, Nheu TV, Simpson RJ, Zhu HJ. Single live cell TGFβ signalling imaging: breast cancer cell motility and migration is driven by sub-populations of cells with dynamic TGFβ-Smad3 activity. Mol Cancer 2015;14:50.
28. Luwor RB, Wang B, Nheu TV, Iaria J, Tsantikos E, Hibbs ML, *et al*. New reagents for improved *in vitro* and *in vivo* examination of TGFβ signalling. Growth Factors 2011;29:211-8.
29. Persson U, Izumi H, Souchelnytskyi S, Itoh S, Grimsby S, Engström U, *et al*. The L45 loop in type I receptors for TGFβ family members is a critical determinant in specifying Smad isoform activation. 1998;434:83-7.
30. Drabsch Y, He S, Zhang L, Snaar-Jagalska BE, ten Dijke P. Transforming growth factor-β signalling controls human breast cancer metastasis in a zebrafish xenograft model. Breast Cancer Res 2013;15:R106.
31. Afrakhte M, Morén A, Jossan S, Itoh S, Sampath K, Westermark B, *et al*. Induction of inhibitory Smad6 and Smad7 mRNA by TGFβ family members. Biochem Biophys Res Commun 1998;249:505-11.
32. Luwor R, Baradaran B, Taylor L, Iaria J, Nheu T, Amiry N, *et al*. Targeting Stat3 and Smad7 to restore TGFβ cytostatic regulation of tumor cells *in vitro* and *in vivo*. Oncogene 2013;32:2433-41.
33. Spiekerkoetter E, Tian X, Cai J, Hopper RK, Sudheendra D, Li CG, *et al*. FK506 activates BMPR2, rescues endothelial dysfunction, and reverses pulmonary hypertension. J Clin Invest 2013;123:3600-13.
34. Wang T, Li BY, Danielson PD, Shah PC, Rockwell S, Lechleider RJ, *et al*. The immunophilin FKBP12 functions as a common inhibitor of the TGFβ family type I receptors. Cell 1996;86:435-44.
35. Chen H, Zhu G, Li Y, Padia RN, Dong Z, Pan ZK, *et al*. Extracellular signal-regulated kinase signaling pathway regulates breast cancer cell migration by maintaining slug expression. Cancer Res 2009;69:9228-35.
36. Kim MY, Oskarsson T, Acharyya S, Nguyen DX, Zhang XH, Norton L, *et al*. Tumor self-seeding by circulating cancer cells. Cell 2009;139:1315-26.
37. Dituri F, Cossu C, Mancarella S, Giannelli G. The interactivity between TGFβ and BMP signaling in organogenesis, fibrosis, and cancer. Cells 2019;8:1130.
38. Kretzschmar M, Doody J, Massagué J. Opposing BMP and EGF signalling pathways converge on the TGFβ family mediator Smad1. Nature 1997;389:618-22.
39. Goumans MJ, Valdimarsdottir G, Itoh S, Lebrin F, Larsson J, Mummery C, *et al*. Activin receptor-like kinase (ALK)1 is an antagonistic mediator of lateral TGFβ/ALK5 signaling. Mol Cell 2003;12:817-28.

40. Oshimori N, Fuchs E. Paracrine TGFβ signaling counterbalances BMP-mediated repression in hair follicle stem cell activation. Cell Stem Cell 2012;10:63-75.
41. Rosen MK, Standaert RF, Galat A, Nakatsuka M, Schreiber SL. Inhibition of FKBP rotamase activity by immunosuppressant FK506: twisted amide surrogate. Science 1990;248:863-6.
42. Wang DJ, Zhi XY, Zhang SC, Jiang M, Liu P, Han XP, *et al*. The bone morphogenetic protein antagonist Gremlin is overexpressed in human malignant mesothelioma. Oncol Rep 2012;27:58-64.
43. Shin K, Lim A, Zhao C, Sahoo D, Pan Y, Spiekerkoetter E, *et al*. Hedgehog signaling restrains bladder cancer progression by eliciting stromal production of urothelial differentiation factors. Cancer Cell 2014;26:521-33.
44. Wu C K, Juang G D, Lai HC. Tumor regression and preservation of graft function after combination with anti-PD-1 immunotherapy without immunosuppressant titration. Ann Oncol 2017;28:2895-6.
45. Peiffer BJ, Qi L, Ahmadi AR, Wang Y, Guo Z, Peng H, *et al*. Activation of BMP signaling by FKBP12 ligands synergizes with inhibition of CXCR4 to accelerate wound healing. Cell Chem Biol 2019;26:652-61.

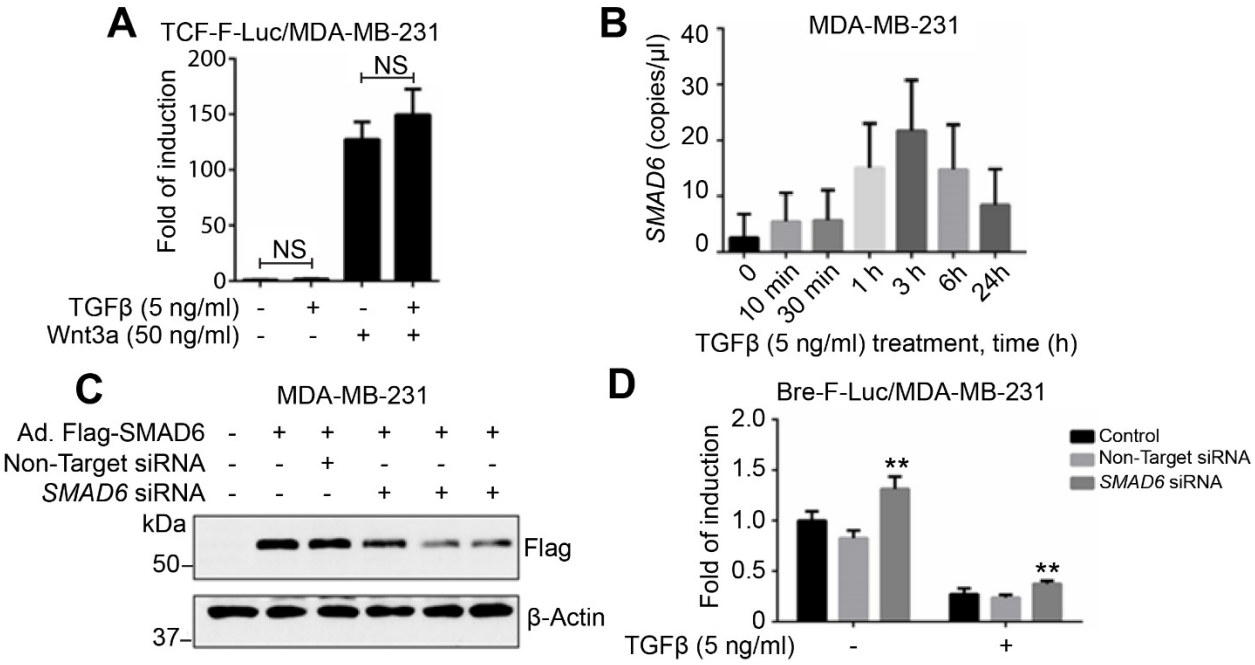

Supplementary Figure 1, related to Figure 1. A, Wnt signaling transcriptional reporter (Ad-TCF-F (firefly)-Luc) assay in response to TGFβ or Wnt3a alone, or combination stimulation in MDA-MB-231 cells. The results are expressed as the mean ± s.d, n = 3. Student's t test, NS, not significant. **B**, Droplet digital PCR to determine the kinetic expression level of *SMAD6* to TGFβ stimulation (5 ng/ml) in MDA-MB-231 cells. The results are expressed as the mean ± s.d, n = 3. **C**, siRNA-mediated knockdown of SMAD6 was measured by western blotting. SMAD6 overexpressed MDA-MB-231 cells were seeded into 6-well plate and transfected with indicated amount of *SMAD6* siRNA. β-Actin was used as an internal control. **D**, TGFβ-inhibited SMAD1/5 signaling (Ad-Bre-F-Luc) could be slightly restored by SMAD6 knockdown in MDA-MB-231 cells. The value is normalized to G-Luc activity. The results are expressed as the mean ± s.d, n = 3. Student's t test, $^{**}P \leq 0.01$.

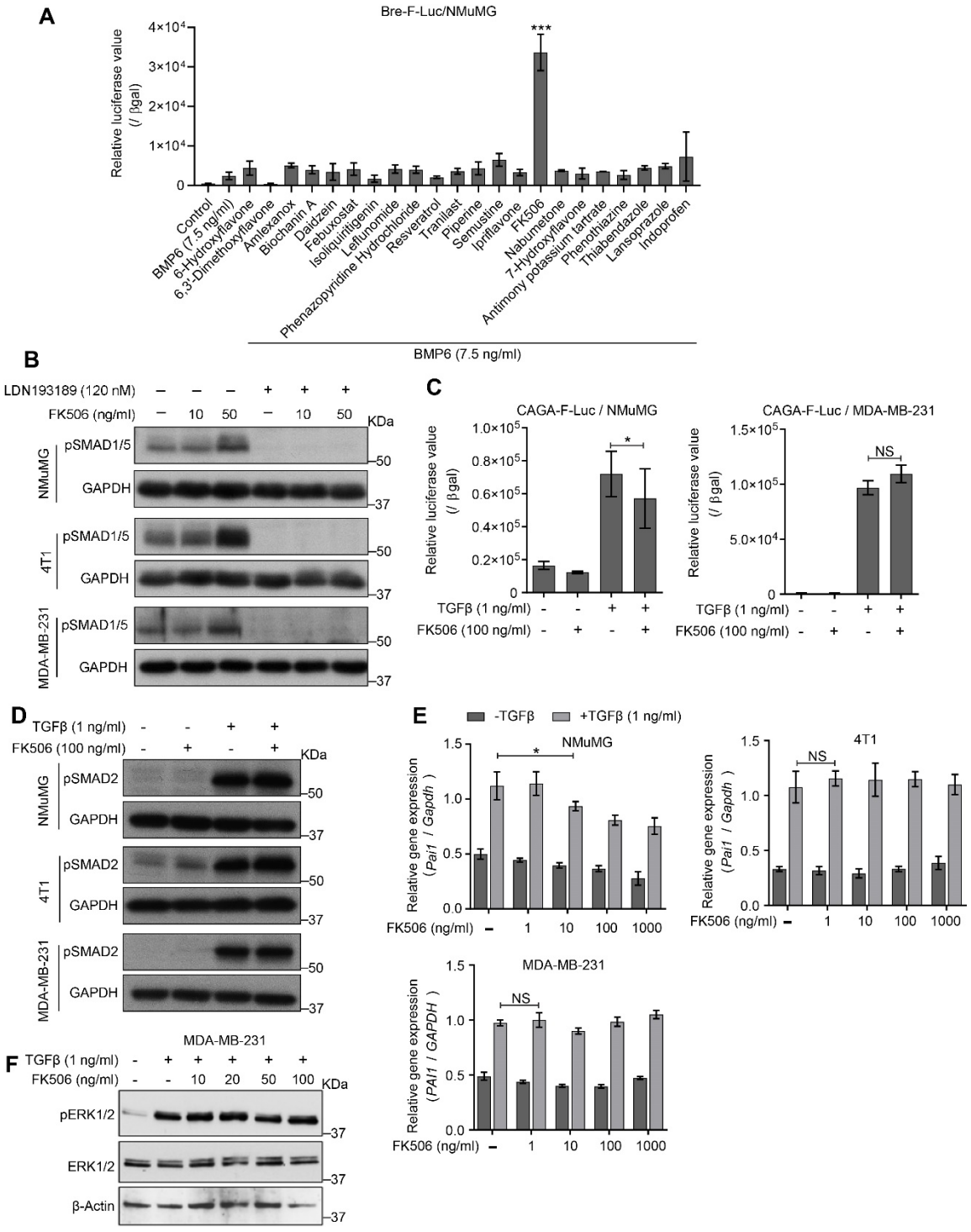

Supplementary Figure 2, related to Figure 3. A, BMP agonist screening in a panel of FDA-approved drugs and bioactive compounds by using Bre-F(firefly)-Luc transcriptional reporter assay. The value is normalized to βgal activity. The results are expressed as the mean ± s.d, n = 3. Student's *t* test, ***$P \leq$ 0.001. **B**, BMP type I receptors inhibitor LDN193189 blocks enhancement of FK506 on SMAD1/5 phosphorylation (pSMAD1/5). GAPDH is used as a loading control. Cells were maintained in 10% serum

medium when receiving treatment. **C**, CAGA-F-Luc reporter assay in NMuMG or MDA-MB-231 cells. The results are expressed as the mean ± s.d, n = 3. Student's t test, NS, not significant, **P* ≤ 0.05. **D**, Western blotting to detect SMAD2 phosphorylation (pSMAD2) in NMuMG, or 4T1, or MDA-MB-231 cells after FK506 or/and TGFβ treatment. GAPDH is used as a loading control. **E**, Expression of TGFβ signaling target genes, *Pai1* in NMuMG, or 4T1 cells, *PAI1* in MDA-MB-231 cells after FK506 or/and TGFβ treatment. *Gapdh* or *GAPDH* is used as an internal control. The results are expressed as the mean ± s.d, n = 3. Student's t test, NS, not significant. **P* ≤ 0.05. **F**, FK506 fails to inhibit TGFβ-mediated activation of MAPK/ERK signaling. ERK1/2 phosphorylation (pERK1/2) was determined by western blotting. β-Actin is used as a loading control.

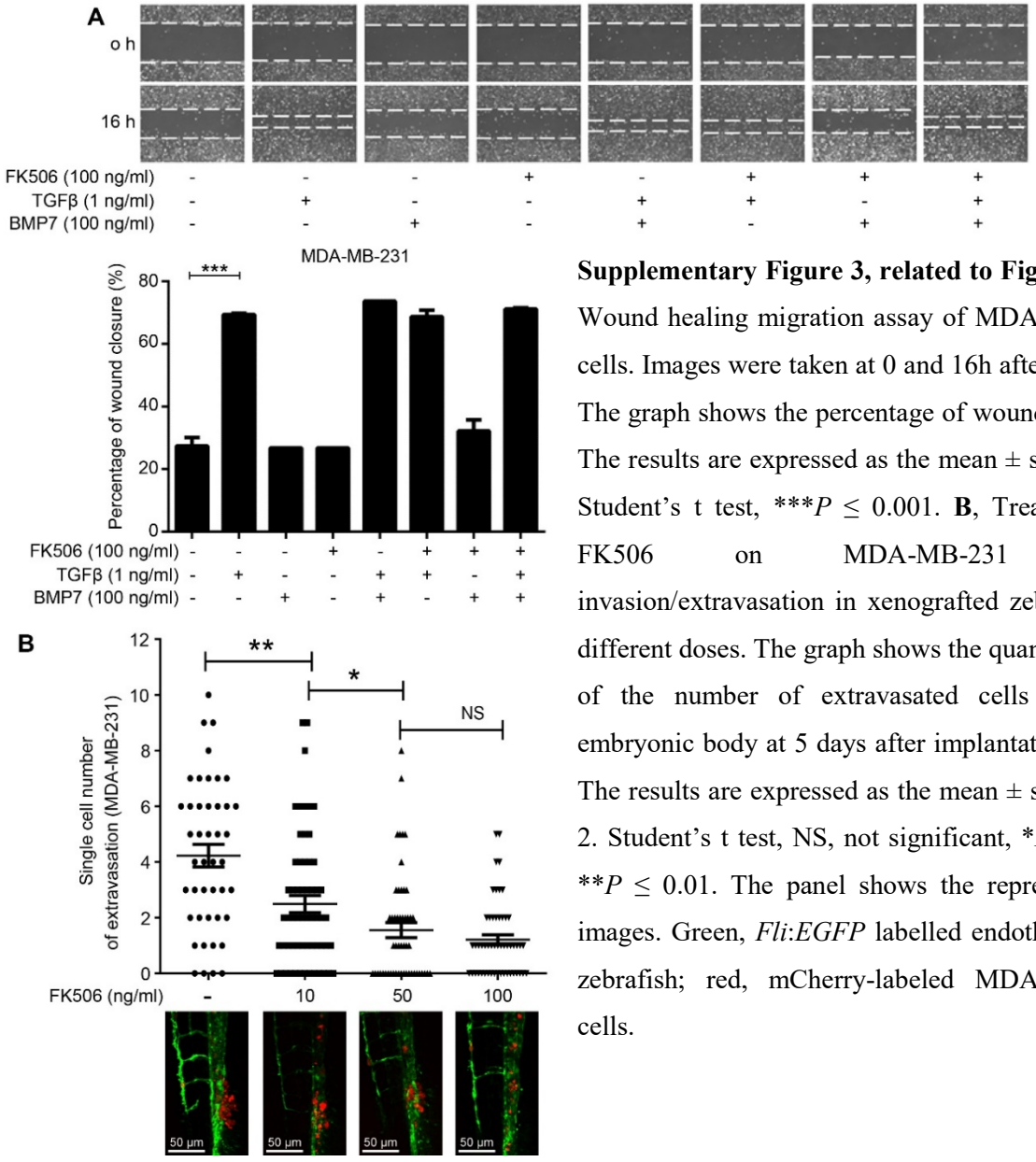

Supplementary Figure 3, related to Figure 5. A, Wound healing migration assay of MDA-MB-231 cells. Images were taken at 0 and 16h after scratch. The graph shows the percentage of wound closure. The results are expressed as the mean ± s.d, n = 3. Student's t test, ****P* ≤ 0.001. **B**, Treatment of FK506 on MDA-MB-231 cells invasion/extravasation in xenografted zebrafish at different doses. The graph shows the quantification of the number of extravasated cells in each embryonic body at 5 days after implantation (dpi). The results are expressed as the mean ± s.e.m, n = 2. Student's t test, NS, not significant, **P* < 0.05, ***P* ≤ 0.01. The panel shows the representative images. Green, *Fli*:*EGFP* labelled endothelium of zebrafish; red, mCherry-labeled MDA-MB-231 cells.

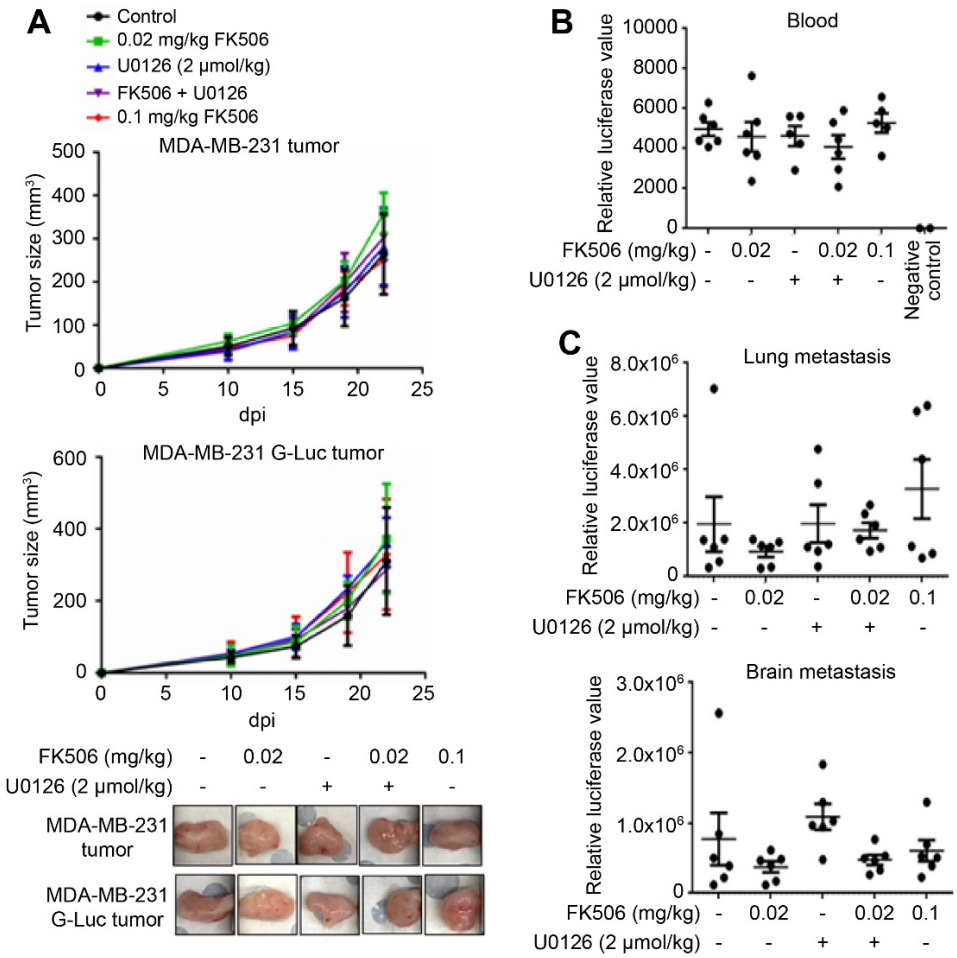

Supplementary Figure 4, related to Figure 6. A, FK506 and U0126 combination treatment has limited effect on primary tumor growth. Graph shows tumor volume of unlabeled MDA-MB-231 and MDA-MB-231-G (Gaussia)-Luc at the indicated days after treatment (dpi). The panel is representative figures of tumors in different groups at day 25 when the mice were sacrificed. **B**, G-Luc value in 5μl of the blood samples of sacrificed mice. Blood from mice without MDA-MB-231-G-Luc tumor implantation was used as a negative control (NC). **C**, Lungs and brains from sacrificed mice were collected and lysed for metastasis analysis by G-Luc activity assay.

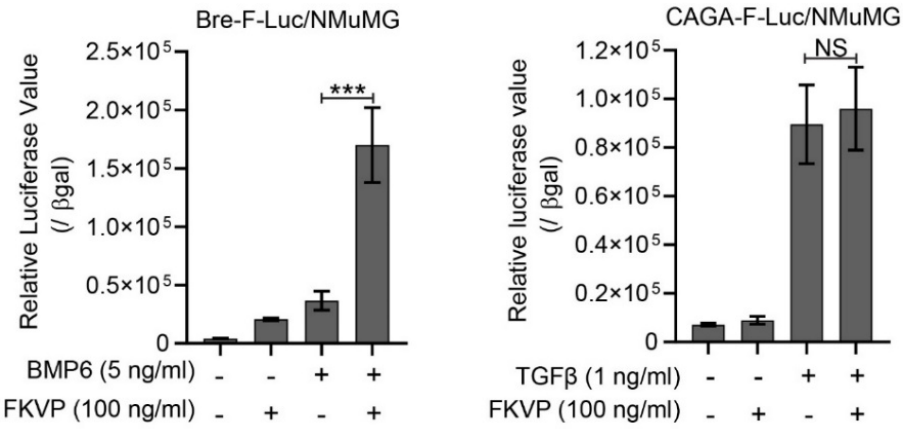

Supplementary Figure 5. FK506 analog FKVP shows significant potential in enhancing BMP signaling by Bre-F(firefly)-Luc reporter assay in NMuMG cells, while TGFβ signaling is not affected by CAGA-F (firefly)-Luc assay. The results are expressed as the mean ± s.d, n = 3. Student's t test, NS, not significant, ***$P \leq 0.001$.